Proceedings 10th NUMGE 2023
10th European Conference on Numerical Methods in Geotechnical Engineering
Zdravkovic L, Kontoe S, Taborda DMG, Tsiampousi A (eds)

https://doi.org/10.53243/NUMGE2023-51

Recent developments of the Particle Finite Element Method (PFEM) in Geomechanics

A. Gens[1], L. Monforte[2], M. Arroyo[1], J.M. Carbonell[3]

[1]*Universitat Politècnica de Catalunya (UPC) - CIMNE, Barcelona, Spain*
[2]*Centre Internacional de Mètodes Numèrics en Enginyeria (CIMNE), Barcelona, Spain*
[3]*Universitat de Vic – Universitat Central de Catalunya (UVic-UCC)- CIMNE, Vic, Spain*

ABSTRACT: The paper presents some recent developments in the formulation of G-PFEM, the Particle Finite Element Method intended for geotechnical applications involving large displacements, finite strains and, often, soil-structure interaction. The associated computer code has been developed and implemented in KRATOS, an object-oriented multi-disciplinary open-access platform. After describing the basic features of the generic PFEM, stabilized mixed formulations for single phase and two-phase materials, required by the use of low-order finite elements, are presented. A nonlocal integration regularization scheme, implemented to deal with materials exhibiting softening behaviour, is described. Two sources of softening are considered: degradation of structured soils and undrained flow liquefaction, requiring different forms of constitutive models. Two examples of application involving softening materials are presented: a biaxial test and a cone penetration test with pore pressure measurements. The integration of the constitutive laws in a large-strain setting and the incorporation of the IMPLEX algorithm are also briefly addressed.

Keywords: PFEM; large deformations; mixed formulation; softening; nonlocal integration

1 INTRODUCTION

Problems involving large strains and large displacements are frequently encountered in geotechnical engineering; they are frequently associated with materials undergoing failure at least in some parts of the domain. Very characteristic examples are the cases that involve the penetration of a rigid object into the ground as occurs in many types of offshore foundations, in cone or other penetration tests for soil characterization, in sampling operations or in the installation of driven piles.

The numerical analysis of these type of problems is challenging and a number of specific numerical techniques have been developed to tackle them such as the Material Point Method, MPM (e.g. Coetzee et al., 2005) and various forms of the Arbitrary Lagrangian Eulerian formulation (Donea et al. 2004) like the Remeshing and Interpolation Technique by Small strain RITTS (e.g. Hu and Randolph, 1998), the Coupled Eulerian-Lagrangian, CEL (e.g. Walker and Yu, 2006) or the efficient ALE approach (e.g. Nazem et al., 2006).

This paper deals with a different numerical technique: The Particle Finite Element Method (PFEM) that is well suited for problems involving not only large strains and displacements but intermittent separation/fusion of bodies as well. It involves frequent remeshing and, generally, the use of low-order elements. The method was initially developed to address fluid-structure interaction problems (Oñate et al., 2004) and subsequently expanded to other fields, like solid-solid interaction, erosion and thermo-plastic problems. It is noteworthy that S.W. Sloan made significant contributions to the method (Zhang et al. 2017, 2018).

Early geomechanical applications of the method include tool-rock interaction problems (Carbonell et al. 2013), the simulation of the cone penetration test (Gens et al. 2016) and the simulation of flow slides (Zhang et al., 2015) where the ground is generally considered as a single-phase material. In this geotechnical context, a new computer code, G-PFEM, has been developed and implemented in KRATOS (Davdand et al. 2010), an object-oriented multi-disciplinary open-access platform for numerical analysis tool development. Extensive improvements of the PFEM method have been required to extend the range of application to the full scope of geotechnical conditions and to enhance the performance, efficiency and robustness of the numerical tool.

After summarising the basic features of the PFEM numerical procedure, this paper reviews briefly some of the novel features of the code: stabilized mixed formulations, nonlocal regularization, the integration of constitutive models in a large-strain setting and the incorporation of the IMPLEX algorithm. Some examples of application involving softening behaviour are presented for illustration.

2 THE PARTICLE FINITE ELEMENT METHOD

PFEM is a continuum method where the solution of the governing set of equations is obtained from a finite element mesh constructed with well-shaped low order elements. The nodes discretizing the analysis domain are considered as material particles that carry mass and state variables. Their movements, computed by the FEM calculation, are tracked throughout the analysis.

The basic sequence follow by the PFEM method is illustrated in Figure 1 and can be defined by the following steps:

1. Begin the computation at each time step with a cloud of points defining the domain of analysis (C^n)

2. Identify the boundaries of the domain of analysis as they can be very distorted and/or new boundaries may be created or suppressed (V^n). The α-shape method (Edelsbrunner and Mucke, 1994) is used for this purpose.

3. Discretize the analysis domain with a finite element mesh (M^n). This may include the introduction of new particles in areas with large plastic deformation, retessellation and some post-tessellation mesh smoothing.

4. State variables are interpolated from the previous mesh to the new one.

4. Solve the governing equations in a Lagrangian formulation and update the state variables in the new configuration

6. Move the points to the new positions resulting from the analysis (C^{n+1})

7. Go back to step 2 and repeat

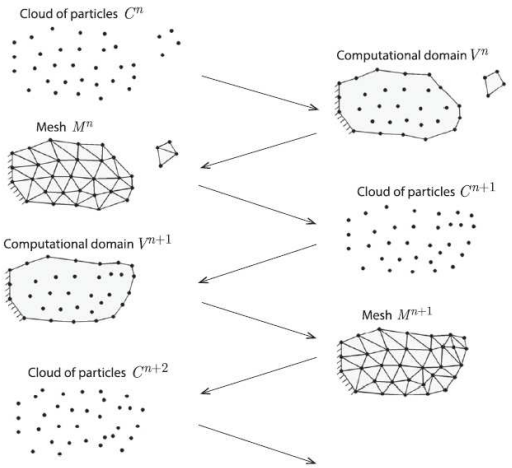

Figure 1. Scheme of a PFEM computation

The quality of the discretization is maintained by constant remeshing by re-triangulation based on Delaunay tessellations. In addition, new particles are added in areas of high gradients of plastic dissipation or water flow occur. Conversely, particles are eliminated if their distance falls below a specified length.

Although not strictly necessary (Zhang et al, 2015), PFEM generally uses low-order finite elements: linear-interpolated triangles in 2D and linear tetrahedrons in 3D. They have a low computational cost; the particles correspond to the mesh nodes and no additional interpolations are required after remeshing. However, as discussed below, these elements entail the use of stabilized mixed formulations.

The accuracy of the solution may be affected by the interpolation of state variables. Although a number of different procedures are available, the nearest point interpolation method has generally been adopted whereby information is directly transferred to the new Gauss points from the closest Gauss point in the previous mesh. In this way, the information is not modified in those finite elements that remain unchanged in the remeshing. In some cases, the SPR (Superconvergent Patch Recovery) interpolation method has been used.

3 STABILIZED MIXED FORMULATIONS

The linear elements used in PFEM are prone to undergo volumetric locking because, at the incompressible limit, they do not satisfy the Babuska-Brezzy conditions. Therefore, stabilized mixed formulations must be implemented. Naturally, the adoption of a mixed formulation increases the number of degrees of freedom per node but the resulting computational cost increase is offset by the simplicity and flexibility associated with the use of linear elements.

Undrained and fully drained geotechnical problems can be analysed considering that the soil or rock is a single-phase material. In that case the governing equation is simply:

$$\nabla \cdot \boldsymbol{\sigma} + \mathbf{b} = \mathbf{0} \tag{1}$$

where $\boldsymbol{\sigma}$ is the Cauchy stress tensor and $\mathbf{b}$ represents the body forces.

The mixed formulation requires an additional scalar governing equation; the following one is used:

$$J - \theta = 0 \tag{2}$$

where $J = \det(\mathbf{F})$ is the determinant of the deformation gradient, $\mathbf{F}$, (also called Jacobian) and θ is the volumetric deformation.

When the Jacobian θ is introduced as a nodal primary variable, the Cauchy stress is determined from a modified deformation gradient where the deviatoric part is prescribed whereas the volumetric part is replaced by the nodal θ variable. In that case, the Cauchy stress tensor depends on both displacements (strains) and the Jacobian, θ. It has been found that the performance of this mixed formulation is better than one based on the Cauchy pressure, p (Monforte et al. 2017a, 2017b).

The stabilisation method used is the Polynomial Pressure Projection, PPP (Dohrmann and Bochev, 2004), applied to the scalar equation (2). In contrast to other stabilization methods, the PPP does not require a mesh-dependent stabilization parameter or the computation of

higher order derivatives and it can be implemented at element level.

A general formulation able to tackle the full range of geotechnical situations, from undrained to fully drained, requires the simultaneous consideration of the mechanical and hydraulic problems in the context of a multiphase material (Monforte et al. 2018). For a saturated soil, the governing equations are:

$$\nabla\cdot\left(\boldsymbol{\sigma}'+p_w\mathbf{I}\right)+\mathbf{b}=\mathbf{0} \tag{3}$$

$$p_w/k_w+\nabla\cdot\mathbf{v}+\nabla\cdot\mathbf{v}^d=\mathbf{0} \tag{4}$$

where $\boldsymbol{\sigma}$' is the effective stress tensor, p_w is the water pressure, $\mathbf{I}$ the identity matrix, k_w water compressibility, $\mathbf{v}$ is the displacement rate, and $\mathbf{v}^d$ Darcy's velocity.

Again, the mixed formulation requires an additional scalar equation; the same one as for the single-phase case is adopted:

$$J-\theta=0 \tag{5}$$

The same considerations regarding the determination of the Cauchy stresses apply as in the single-phase case above.

Stabilization of the formulation is also achieved by the PPP procedure applied now to the two scalar equations (4) and (5). A comparison of different mixed formulations and stabilization procedures applied to various single-phase and two-phase problems has been presented in Monforte et al. (2017b); the results support the adoption of the Jacobian nodal variables and the use of the PPP stabilization method. Also, Monforte et al. (2019b) has reported low order stabilized mixed schemes for the full dynamic Biot formulation required in dynamic cases where the fluid acceleration is not negligible compared to that of the solid phase. This generalization is outside the scope of this paper.

4 PFEM FOR SOFTENING MATERIALS

4.1 Constitutive models and formulation

As for any numerical technique, the performance of PFEM analyses involving softening materials entails especial challenges mainly related to mesh dependency and the computability of the solution. Yet, softening materials are worthy of particular attention because they are often associated with excessive deformations and displacements and, on many occasions, with catastrophic failures that occur without warning (Gens, 2019).

Two sources of softening have been examined: structured materials and liquefiable soils. Structured materials such as soft rocks, natural clays or cemented soils exhibit higher strength and stiffness due to bonding, the physical nature of which may be quite varied. Softening arises from the weakening of the bonds due to plastic straining or to a variety of environmental factors such as temperature or weathering. From the constitutive point of view (Gens and Nova 1988), their behaviour may be visualized by an outer yield locus that degrades towards the smaller intrinsic yield surface as restructuration progresses (Figure 2a). This results in the softening behaviour at low stresses shown in Figure 2b.

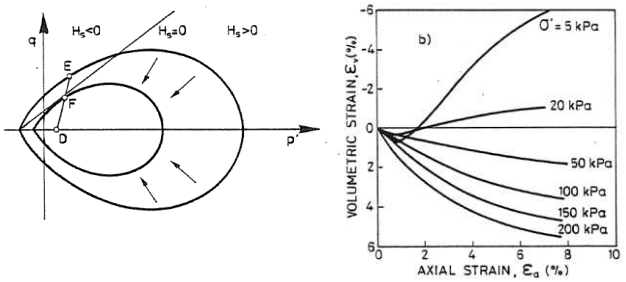

a) b)

Figure 2. Constitutive model for structured soils. a) Initial and intrinsic yield loci b) Stress-strain curves

The softening mechanism is different in soils undergoing flow liquefaction. Under undrained conditions, the very open fabric of the material collapses after reaching a peak well away from the drained failure envelope. After the collapse, the soil reaches a critical state condition at a much lower value of undrained shear strength. This behaviour can be captured by a constitutive model such as CASM (Yu, 1998) that incorporates a yield locus with and appropriate shape (Figure 3).

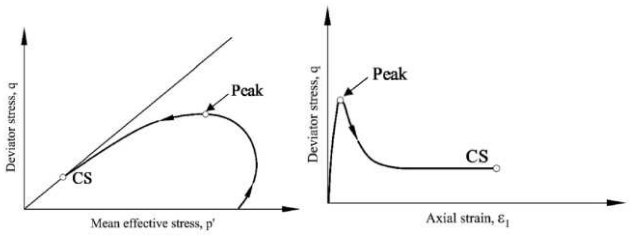

a) b)

Figure 3. Constitutive model for liquefiable soils. a) Yield locus b) Stress-strain curve

The mitigation of the pathological mesh dependence of the analyses involving softening requires the use of a regularisation technique incorporating a fixed length scale. In the PFEM code presented here, the nonlocal integral technique has been adopted. Because it does not change the governing equations, the implementation is reasonably straightforward (Mánica et al. 2018).

The method implies that the constitutive model is evaluated at each Gauss point using one or more nonlocal variables instead of considering only the Gauss point itself. The nonlocal variable is determined as:

$$\bar{\beta}(\mathbf{x})=\frac{\int_\Omega w(\mathbf{x},\|\mathbf{y}-\mathbf{x}\|)\beta(\mathbf{y})d\Omega}{\int_\Omega w(\mathbf{x},\|\mathbf{y}-\mathbf{x}\|)d\Omega} \tag{6}$$

where β is the local variable, $\mathbf{x}$ and $\mathbf{y}$ are coordinates and w is the weighing function that controls the influence of the neighbouring integration points as a function

of their distance to the Gauss point under consideration. Naturally the calculation of the nonlocal variable is done in a discretized form:

$$\bar{\beta}(\mathbf{x}_i) = \frac{\sum_{ij} w(\mathbf{x}_i, \chi_{ij}) \beta(\mathbf{x}_j)}{\sum_{ij} w(\mathbf{x}_i, \chi_{ij})} \tag{7}$$

where χ_{ij} is the distance between Gauss points i and j. For the elastoplastic models outlined above, the nonlocal variables are the hardening parameters although, of course, other choices are possible.

The weighing function proposed by Galavi and Schweiger (2010) is adopted because it has been shown to perform better than other alternatives (Summersgill et al., 2017):

$$w(\mathbf{x}, \chi) = \frac{\chi}{l_c} \exp\left(-\left(\frac{\chi}{l_c} \right)^2 \right) \tag{8}$$

where l_c is a characteristic length. Perhaps unexpectedly, the function has a null value when χ is zero and it reaches a maximum at a distance of $\sqrt{2} l_c / 2$.

From a strict point of view, the nonlocal formulation effectively couples the constitutive response of all the integration points in the analysis domain. Consequently, a very large system of coupled equations would need to be solved in each iteration. In practice, variables are determined using the nonlocal approach at the beginning of each loading increment but, during the subsequent iterations, they evolve independently of their neighbours. Thus, stress integration is performed at each integration point independently of the other Gauss points.

The nonlocal regularisation requires a sufficient number of neighbouring points to be applied effectively and, therefore, there is a natural synergy with the PFEM. Since the failure mechanism is generally not known in advance, analyses using a fixed mesh would require a fine discretization over large areas of the domain. In the PFEM, however, the mesh is intensely discretised in the areas where more plastic strain (and therefore softening) accumulates and, in this way, the required neighbouring points are automatically created only in the areas of the domain where they are required. Indeed, it is reasonable to incorporate the prescribed characteristic length in the criterion for deciding whether new particles are to be generated. Further details on the PFEM formulation for softening materials and associated constitutive laws are presented in Monforte et al. (2019a, 2021).

4.2 Examples of application

The cases presented in this section are computed with the mixed stabilized formulations presented before. The first example refers to the case of a biaxial test performed on a structured soil, so a constitutive law like the one depicted in Figure 2 is used. The test is assumed fully drained, so the single-phase formulation is employed and nonlocal integration is used.

Figure 4a shows the variation of vertical pressure vs vertical shortening for the case where the nonlocal scheme was used whereas Figure 4b presents the results of the equivalent analyses using only local integration. The analyses have been performed using six different initial discretizations ranging from 602 to 20320 nodes. It can be noted that in Figure 4a the differences between the different computation is quite small in contrast with the local integration results of Figure 4b. This latter Figure also shows that some of the analyses experienced numerical difficulties at various stages of the calculations resulting in irregular oscillations. Figure 5 presents the contours of accumulated plastic strains in the analyses performed with nonlocal integration for the six meshes used. It can be noted that the same failure mechanism develops in all cases and that the thickness of the shear band is constant and controlled by the characteristic length used in the analyses.

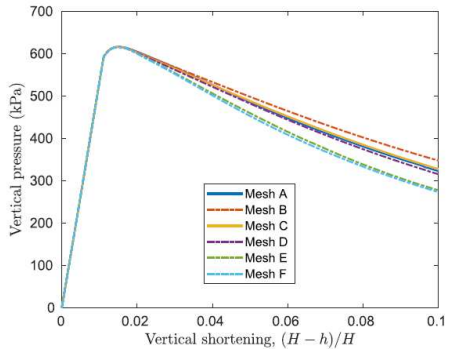

a)

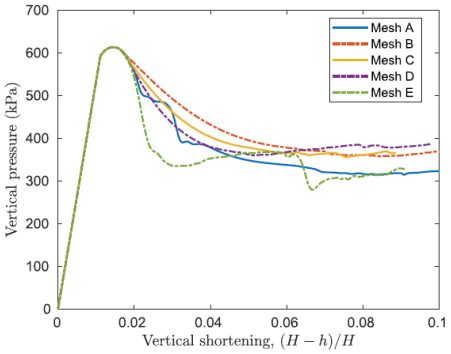

b)

Figure 4. Vertical pressure vs. vertical shortening in a biaxial test on a structured soil. Mesh A is the coarsest discretization and F the finest. a) Nonlocal integration b) Local integration

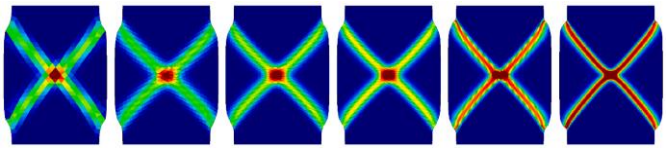

Figure 5. Contours of accumulated plastic deviatoric strain in a biaxial test on a structured soil. The meshes become finer form left to right.

The second example involves the simulation of a CPTU cone penetration test in liquefiable materials. The two-phase mixed stabilised formulation with non-

local integration is used in order to compute pore pressures in a proper manner. The CASM constitutive model (Figure 3) is employed and, given the brittle nature of the soil, nonlocal integration is again used. Eight different analyses have been performed with materials of different brittleness indices ranging from the most brittle soil, A (brittleness index 0.71) to the least brittle one, H (brittleness index 0.08). The peak undrained shear strength is the same in all cases. Cone penetration is performed at the standard rate of 0.02 m/s and the soil permeability has been chosen to ensure undrained conditions throughout.

The contours of pore pressure and mean stress at steady state penetration are shown in Figures 6 and 7, respectively, for the two extreme cases of brittleness, A and H. It can be noted that pore pressures are similar but the effective mean stresses along the cone are much lower in the brittle case because of the undrained collapse undergone by the soil. The similarity of the pore pressures arises from the fact that they are controlled by the large increases in total stresses that are similar in all cases (Monforte et al. 2021). Figure 8 shows the results of the analyses in terms of the parameters typically recorded in the CPTU test: net cone resistance and pore pressure measured at the cone shoulder. Again, pore pressures are similar, but the net cone resistance is much lower in the brittle material in spite of the fact that the peak undrained shear strength is the same in all cases.

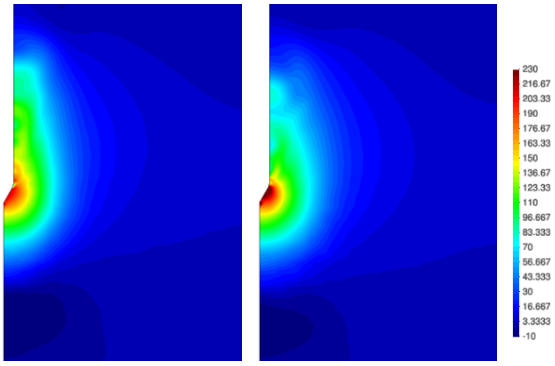

a) b)

Figure 6. Contours of pore pressure in the CPTU test. a) Case A, maximum brittleness, b) case H, minimum brittleness

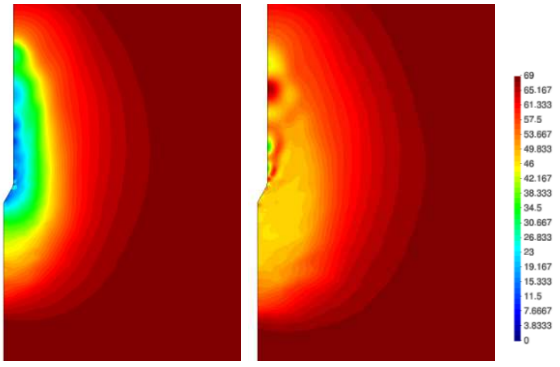

a) b)

Figure 7. Contours of effective mean stresses in the CPTU test. a) Case A, maximum brittleness, b) case H, minimum brittleness

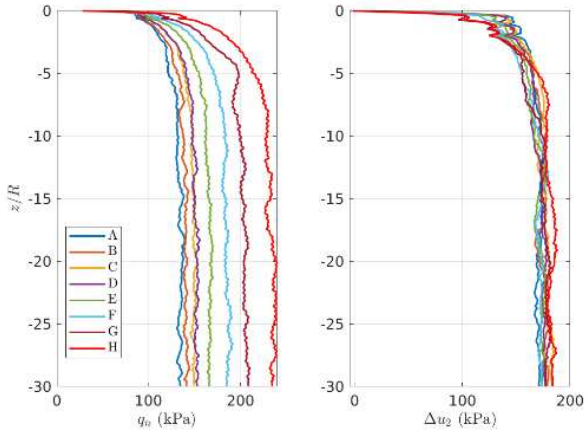

a) b)

Figure 8. Results of the simulation of the CPTU test. a) Net cone resistance, b) Pore pressure measured at the cone shoulder

5 OTHER RECENT DEVELOPEMNTS

Due to space limitations, other recent developments will only be briefly mentioned here. Constitutive model integration has to be performed within a frame invariant framework when large strains are involved that may result in significant rotations. To this end, the elastoplastic models are formulated in terms of a multiplicative decomposition of the total deformation into an elastic and plastic part (Monforte et al., 2015).

To increase the robustness and computability of the PFEM analyses, the IMPLEX integration algorithm (Oliver et. al., 2008) has been recently implemented. It is a two-step solver with a first extrapolation step that computes the boundary value problem using an extrapolated value of the increment of the plastic multiplier followed by a correction step where the constitutive equations are correctly evaluated at each integration point. In this way, the number of iterations reduces drastically at the cost of introducing some error that depends on the size of the time step. In the current implementation, both steps use explicit schemes for the evaluations of the constitutive model (Monforte et al, 2019a).

Although penetration problems generally involve contacts between soil and rigid bodies, the treatment of the contacts has been recently extended to consider the interaction between two deformable bodies (Carbonell et al. 2022).

6 CONCLUSIONS

G-PFEM is a numerical procedure and computer code developed to carry out analyses involving large displacements, large deformations and soil-structure interaction. A number of additional developments are required to enhance the robustness and efficiency of the method, some of which have been briefly reviewed: stabilized mixed formulations, nonlocal regularization, integration of constitutive models in a large-strain setting

and the incorporation of advanced integration algorithms. In the space available, it has only been possible to present two examples of application, involving softening behaviour, that illustrate the successful performance of the PFEM.

7 ACKNOWLEDGEMENTS

The authors thank the support from the Spanish Ministry of Economy and Competitiveness, through the "Severo Ochoa Programme for Centres of Excellence in R&D" (CEX2018-000797-S). The financial support of the Ministry of Science and Innovation of Spain through research grant PID2020-119598RB-I00 is also gratefully appreciated.

8 REFERENCES

Carbonell, J.M., Oñate, E., Suárez, B. 2013. Modelling of tunnelling processes and rock cutting tool wear with the particle finite element method. *Comput Mech* **52**, 607–629.

Carbonell J.M., Monforte, L., Ciantia, M.O., Arroyo, M., Gens, A. 2022. Geotechnical particle finite element method for modeling of soil-structure interaction under large deformation conditions. *Journal of Rock Mechanics and Geotechnical Engineering* **14**, 967-983.

Coetzee, C.J., Vermeer, P.A., Basson, A-H. 2005. The modelling of anchors using the material point method. *Int. J. Num. Anal. Meth. Geomech* **29**:879–95.

Dadvand, P., Rossi, R., Oñate E. 2010. An object-oriented environment for developing finite element codes for multidisciplinary applications. *Arch Comput Methods Eng* **17**:253–97.

Dohrmann, C.R., Bochev, P.B. 2004. A stabilized finite element method for the Stokes problem based on polynomial pressure projections. *Int J Numer Methods Fluids* **46**:183–201

Donea, J., Huerta, A., Ponthot, J.P., Rodríguez-Ferran, A. 2004. *Arbitrary Lagrangian-Eulerian methods*. Encyclopedia of computational mechanics. John Wiley & Sons.

Edelsbrunner, H., Mucke, E.P. 1994. Three dimensional alpha shapes. *ACM Trans Graph* **13**:43–72

Galavi, V., Schweiger H.F. 2010. Nonlocal multilaminate model for strain softening analysis. *Int J Geomech* **10**:30–44

Gens, A. 2019. Hydraulic fills with special focus on liquefaction. *Proc. 17th Europ. Conf. Soil Mech. Geot. Eng.* (Eds Sigursteinsson, H. et al.). 1-31. IGS, Reykjavik.

Gens. A., Arroyo, M. Carbonell, J.M., Ciantia, M.O., Monforte, L., O'Sullivan, C. 2016. Simulation of the cone penetration test: discrete and continuum approaches. *Australian Geomechanics* **51**:169-182.

Gens, A., Nova, R. 1993. Conceptual bases for a constitutive model for bonded soils and weak rocks. *Geotechnical engineering of hard soils–soft rocks*, **1**: 485-494. A.A. Balkema, Rotterdam.

Hu, Y., Randolph, M.F. H-adaptive 1998. FE analysis of elasto-plastic non-homogeneous soil with large deformation. *Comput Geotech* **23**:61–83.

Mánica, M.A., Gens, A., Vaunat, J., Ruiz, D.F. 2018. Nonlocal plasticity modelling of strain localisation in stiff clays. *Comput Geotech* **103**:138–50.

Monforte, L., Arroyo, M., Gens, A., Carbonell, J.M. 2015. Explicit finite deformation stress integration of the elastoplastic constitutive equations. *Proc. 14th Int. IACMAG Conference*. 267–72. Kyoto.

Monforte, L., Arroyo, M., Carbonell, J.M., Gens, A. 2017a. Numerical simulation of undrained insertion problems in geotechnical engineering with the Particle Finite Element Method (PFEM). *Comput Geotech* **82**: 144-156

Monforte, L., Carbonell, J.M., Arroyo, M. and Gens, A. 2017b. Performance of mixed formulations for the Particle Finite Element Method in soil mechanics problems. *Computational Particle Mechanics* **4**: 269-284.

Monforte, L., Arroyo, M., Carbonell, J.M., Gens, A. 2018. Coupled effective stress analysis of insertion problems in geotechnics with the Particle Finite Element Method. *Comput Geotech*, **101**:114–129

Monforte, L., Ciantia, M.O., Carbonell, J.M., Arroyo, M., Gens, A. 2019a. A stable mesh-independent approach for numerical modelling of structured soils at large strains. *Comput Geotech*, **116**: Article number 103215.

Monforte, L., Navas, P., Carbonell, J. M., Arroyo, M., Gens, A. 2019b. Low- order stabilized finite element for the full Biot formulation in soil mechanics at finite strain. *Int. J. Num. Anal. Meth. Geomech*. **43**:1488-1515.

Monforte, L., Gens, A., Arroyo, M., Mánica, M., Carbonell, J.M. 2021. Analysis of cone penetration in brittle liquefiable soils. *Comput Geotech* **134**, paper 104123.

Nazem, M., Sheng, D., Carter, J.P. 2006. Stress integration and mesh refinement for large deformation in geomechanics. *Int J Numer Meth Eng* **65**:1002–27.

Oliver, J., Huespe, A.E., Cante, J.C. 2008. An implicit/explicit integration scheme to increase computability of nonlinear material and contact/friction problems. *Comput Methods Appl. Mech. Eng.* **197**:1865–89.

Oñate, E., Idelsohn, S.R., Del Pin, F., Aubry, R. 2004. The particle finite element method: an overview. *Int J Comput Methods* **1**:267–307.

Summersgill, F.C., Kontoe, S., Potts, D.M. 2017. Critical assessment of nonlocal strain-softening methods in biaxial compression. *Int J Geomech* **17**:04017006.

Walker, J., Yu, H.S. 2006. Adaptive finite element analysis of cone penetration in clay. *Acta Geotech* **1**:43–57.

Yu, H.S. 1998. CASM: A unified state parameter model for clay and sand. *Int. J. Num. Anal. Meth. Geomech* **22**: 621–653.

Zhang, X., Krabbenhoft, K., Sheng, D., Li, W. 2015 Numerical simulation of a flow-like landslide using the particle finite element method. *Comput Mech* **55**:167–177.

Zhang, X., Sheng, D-, Sloan, S.W., Bleyer, J. 2017. Lagrangian modelling of large deformation induced by progressive failure of sensitive clays with elastoviscoplasticity. *Int J Numer Meth Eng* 2017.

Zhang, X., Sloan, S.W., Oñate, E. 2018. Dynamic modelling of retrogressive landslides with emphasis on the role of clay sensitivity. *Int J Numer Anal Methods Geomech* **42**:1806–1822.